

Improved One-dimensional Analysis of CMOS Photodiode Including Epitaxial-Substrate Junction

J. S. Lee, R. I. Hornsey

Dept. of Electrical and Computer Engineering, University of Waterloo, Ontario, Canada
rhornsey@venus.uwaterloo.ca, Tel: (519) 888-4097, FAX: (519) 746-3077

Abstract

An improved one-dimensional analysis of CMOS photodiode has been derived in which the effect of the substrate, which forms a high-low junction with the epitaxial layer, has been included. The fully analytical solution was verified with numerical simulations based on parameters extracted from a standard 0.35 μm CMOS process. The parameter availability and the degree of accuracy for photoresponse modeling are briefly discussed. Two empirical parameters are suggested to offset the unavoidable inaccuracies in the employed parameters. The derived semi-empirical expression exhibits a good agreement with the measured spectral response of $n^+\text{-p}_{\text{epi}}$ photodiodes fabricated using a standard 0.35 μm CMOS process. The simplicity and the accuracy of the model makes it a suitable candidate for implementation in circuit-level simulation of $n^+\text{-p}_{\text{epi}}$ CMOS photodiodes. The applicability of one-dimensional approximation of the peripheral photoresponse in linear- and two-dimensional arrays is also discussed with measurements based on linear photodiode arrays.

I. Introduction

Historically, following the classical one-dimensional analyses of photodiodes and other photovoltaic devices [1-3], subsequent efforts focused on the effects of lateral diffusion in linear and two-dimensional arrays as they were generalized with CCDs. Several studies of lateral diffusion have investigated the edge effect – the peripheral collection of photocarriers along the lateral edge of the photodiode – also known as peripheral photoresponse or lateral photocurrent [4-12]. Other studies of lateral diffusion have dealt with the lateral crosstalk – the unwanted component of lateral current consisting of stray photocarriers that have diffused out of the pixel site from which they have originated – suggesting a number of ways to minimize this effect [13-19]. A number of publications provided the analysis of the effect of lateral crosstalk on the modulation transfer function (MTF) of the imaging array [1,13-16]. Several researchers have also proposed a definition

termed cross-responsivity, which employs lateral diffusion from excitation of a single photodiode to characterize the lateral diffusion an array of photodiodes, analogous to impulse response of a linear time-invariant system [16-19]. Notwithstanding the importance of multi-dimensional effects such as lateral diffusion, however, we have considered one-dimensional effects particular to CMOS technology, such as the high-low doped junction between the epitaxial layer and the substrate, which has not been extensively treated in the literature [15].

II. One-Dimensional Analysis

Fig. 1 shows the measured spectral response obtained from an $n^+\text{-p}_{\text{epi}}$ photodiode fabricated on a standard 0.35 μm nwell process and the theoretical transmission coefficient, $(1-R)$, of a single amorphous silicon dioxide overlayer, fitted to the observed interference pattern in the measured spectral response. It can be observed that optical reflection is responsible for a significant loss of incident photons.

Given that the substrate is generally more heavily doped than the epitaxial layer, the resulting electric field causes the drift of photocarriers from the substrate bulk to the epitaxial layer. If we neglect the substrate contribution, however, the maximum possible internal quantum efficiency of epitaxial layer for now is simply the integration of all optical generation occurring within the epitaxial layer thickness, t , i.e.

$$\eta = \int_0^t \exp(-x/L_{op}) dx = 1 - \exp(-t/L_{op}) \quad (1)$$

Fig. 2 shows a comparison of the measured spectral response with the expression in (1) multiplied by the previously obtained values of $(1 - R)$. The thickness of the epitaxial layer (3.0 μm) was estimated using an scanning electron microscope. From the comparison it can be observed that the epitaxial layer alone cannot account for all of the measured photoresponse, especially in the long-wavelength regions of the visible spectrum where the substrate contribution is expected to be the largest. Consider Fig. 3 depicting the one-dimensional structure of $n^+\text{-p}_{\text{epi}}$

type photodiode. We assume that the epitaxial layer is characterized by thickness t , a uniform doping concentration N_e , and a diffusion length L_e . The substrate is characterized by a different doping concentration N_s , and diffusion length L_s . The depletion region of the photodiode penetrates the epitaxial layer to a depth, d , below the surface. The proposed boundary conditions for the excess carrier density in the epitaxial layer are

$$\hat{n}_e(x=d) = 0 \quad (2)$$

and

$$\left. \frac{\partial \hat{n}_e}{\partial x} \right|_{x=t} = \Phi_s, \quad (3)$$

where Φ_s is the flux of excess minority carriers injected into the epitaxial layer which have originated from the substrate and the high-low junction. As for the substrate [15],

$$\hat{n}_s(t) = \hat{n}_e(t) \frac{N_e}{N_s} \quad (4)$$

and

$$\hat{n}_s(x) \rightarrow 0 \text{ as } x \rightarrow \infty. \quad (5)$$

The expression for Φ_s was solved by introducing the relation,

$$\Phi_s = D_s \left. \frac{\partial \hat{n}_s}{\partial x} \right|_{x=t} = D_e \left. \frac{\partial \hat{n}_e}{\partial x} \right|_{x=t} \quad (6)$$

by assuming that the generation within the high-low doped junction is negligible. The resulting excess carrier density distribution in the epitaxial layer aided by the substrate contribution, n_e , and the corresponding diffusion-based photocurrent at the photodiode junction is shown in Fig. 4.

However, as illustrated in Fig. 5, calculations showed that the boundary condition (4), used in determining the excess carrier distribution in the substrate, may be effectively approximated by

$$\hat{n}_s(t) = 0 \quad (7)$$

when the substrate is doped significantly higher than the epitaxial layer ($N_s/N_e > 10$). Following the above approximation, the expression of photocurrent simplifies to that shown in Fig. 4. It can be observed that in the limiting case where $L_s \ll L_{op}$ the derived expression of quantum efficiency reduces to the case with zero net flux from the substrate ($\Phi_s = 0$), as expected. In the other limiting case where $L_s \gg L_{op}$ the expression reduces to

$$\eta = (1-R) \exp(-d/L_{op}) \quad (8)$$

which characterizes 100% collection efficiency for all optical generation below the photodiode junction depth. Numerical simulations were employed to verify the derived photocurrent expression in which a set of parameters based on the 0.35 μm process were adopted.

III. Suggested Empirical Parameters

The comparison of the derived quantum efficiency expression with experimental data requires several material parameters that are not accurately known, including the minority carrier lifetime in the substrate. Given that the minority carrier diffusion coefficient and the minority carrier lifetime of the substrate are not generally characterized, we have replaced the substrate diffusion length in the analytical model with an empirical parameter, $L_{s, \text{fitted}}$, as a matter of convenience. Fig. 6 shows the result of fitting the substrate diffusion length to the measured spectral response. The substrate diffusion length of $L_{s, \text{fitted}} = 4.0 \mu\text{m}$ was extracted from the best fit; this is a reasonable value since the divergence of the measured quantum efficiency from the theoretical curve of $(1-R)$ indicates that L_s is not considerably larger than $(L_{op} - t)$, which is approximately $6.7 - 3.0 = 3.7 \mu\text{m}$ at 660 nm.

The divergence of the theoretical expression from the measured spectral response at the short-wavelength end of the spectrum (in Fig. 7) is due to the optical generation in the photodiode depletion region and the diffusion current in the “n+” quasi-neutral region. Assuming that no recombination takes place in the depletion region of the photodiode, the optical generation can be incorporated into the analysis simply by adding the integration of optical generation within the depletion region. This simply results in an expression where the junction depth, d , is replaced by $(d-w)$ where w is the width of the photodiode depletion region.

However, the extraction of the junction depth and the doping concentrations by which the depletion width may be calculated have to be extremely precise in order to yield an accurate short-wavelength response: the optical absorption distance for 400 nm light is only about 80 nm so that inaccurate calculation of $(d-w)$ by 10 nm causes the short-wavelength to vary by about 10%. While the metallurgical junction depth may be extracted at the level of the

required accuracy, the determination of the depletion width is complicated by the fact that the doping density of the epitaxial layer near the surface is controlled by the threshold voltage adjustment implant, which is not generally characterized in terms of the final value near the surface. Hence, as a matter of convenience, $(d-w)$ is simply replaced by empirical parameter d_{fitted} in the final expression shown below:

$$J_{ph} = qG_oL_{op} \left(\exp(-d_{\text{fitted}}/L_{op}) - L_{op} \exp(-t/L_{op}) \left(\frac{L_{s,\text{fitted}} - L_{op}}{L_{s,\text{fitted}}^2 - L_{op}^2} \right) \right) \quad (9)$$

where

$$G_o = P_{in} \frac{\lambda}{hc} (1 - R(\lambda)) \quad (10)$$

P_{in} is the incident power density, λ is the wavelength, h is plank's constant, and c is the speed of light.

The parameter, d_{fitted} , denotes the effective junction depth at which the derived expression, based the epitaxial layer and the substrate photocurrent, can be adapted to accurately follow the measured photoresponse at the short wavelength end of the visible spectrum. This parameter also empirically incorporates the effect of surface recombination, which significantly affects the short-wavelength response of the photodiode. We have found that the empirical parameter d_{fitted} provides a good fit to the measured data at the short-wavelength regions of the visible spectrum although the theoretical photocurrent contribution of the n+ quasi-neutral region does not conform to the aforementioned empirical fitting $\exp(-d/L_{op})$. Fig. 8 shows the result of the empirical fitting at $L_{s,\text{fitted}} = 4.0 \mu\text{m}$ and $d_{\text{fitted}} = 50 \text{ nm}$. Note that the reported metallurgical junction depth was 100 nm. From Fig. 8, it can be seen that the semi-empirical expression provides a reasonable fit to the measured spectral response. An improved model of optical reflections in CMOS overlayers appears necessary in order to further minimize the remaining discrepancies.

IV. Summary:

In summary, a fully analytical derivation of CMOS photodiode quantum efficiency was introduced. Two empirical parameters were suggested as a practical alternative to the parameter extractions that need to be highly precise.

V. Acknowledgements

The authors gratefully acknowledge the financial support from Mitel Corp. and Canada's Network of Centres of Excellence. The fabrication and support services from Canadian Microelectronics Corporation is also acknowledged for enabling this research.

- [1] M.H. Crowell and E.F. Labuda, *Bell Syst. Techn. J.*, vol. 48, 1969, pp.1481-1528
- [2] F. van de Wiele, *Photodiode quantum efficiency*, in *Solid State Imaging*, P.G. Jespers, F. van de Wiele, and M.H. White, Eds. Leydon: Norrdhoff, 1976, pp. 47-90
- [3] J. Geist, and H. Baltes, *Applied Optics*, vol. 28, no. 18, 1989, pp. 3929-3939
- [4] J. Shappir, and A. Kolodny, *IEEE Trans. Electron Devices*, vol. ED-24, no. 8, 1977, pp. 1093-1097
- [5] T.I. Kamins and G.T. Fong, *IEEE Trans. Electron Devices*, vol. ED-25, 1978, pp.154-159
- [6] H. Holloway, *J. Appl. Phys.*, vol. 49. no. 7, 1978, pp. 4264-4269
- [7] S. Kirkpatrick, *IEEE Trans. Electron Devices*, vol. ED-26, 1979, pp. 1742-1753
- [8] H. Holloway, and A.D. Brailsford, *J. Appl. Phys.*, vol. 55, no. 2, 1984, pp. 446-453
- [9] A.D. Brailsford and H. Holloway, *J. Appl. Phys.*, vol. 56, no. 4, 1984, pp. 1008-1011
- [10] H. Holloway, and A.D. Brailsford, *J. Appl. Phys.*, vol. 54, no. 8, 1983, pp. 4641-4656
- [11] L.M. Sander, *J. Appl. Phys.*, vol. 57, no. 6, 1985, pp. 2057-2059
- [12] H. Holloway, *J. Appl. Phys.*, vol. 60, no. 3, 1986, pp. 1091-1096
- [13] F.C. Elliot, *IEEE Trans. Electron Devices*, vol. ED-21, 1974, pp.613-616
- [14] D.H. Seib, *IEEE Trans. Electron Devices*, vol. ED-21, 1974, pp. 210-217
- [15] M.M. Blouke and D.A. Robinson, *IEEE Trans. Electron Devices*, vol. ED-28, 1981, pp. 251-256
- [16] J.P. Lavine, E.A. Trabka, B.C. Burkey, T.J. Tredwell, E.T. Nelson, and C.N. Anagnostopoulos, *IEEE Trans. Electron Devices*, vol. ED-30, 1983, pp. 1392-1394
- [17] D. Levy and S.E. Schacham, *IEEE Trans. Electron Devices*, vol. ED-34, no. 10, 1987, pp. 2059-2069
- [18] D. Levy, S.E. Schacham, and I. Kidron, *IEDM*, 1986, pp. 373-376
- [19] D. Levy, and S.E. Schacham, *J. Appl. Phys.*, vol. 64, no. 10, 1988, pp. 5230-5233
- [20] E.D. Palik, e.d., *Handbook of Optical Constants of Solids*, Academic Press, 1985

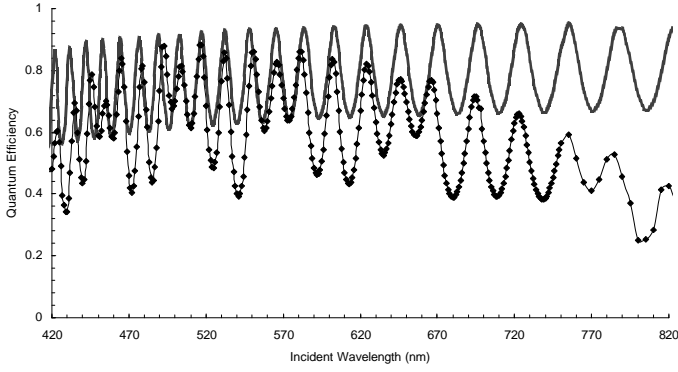


Fig. 1. (a) Measured external quantum efficiency of n^+p_{epi} photodiode – thin line with data points; (b) $(1-R)$ of single layer of amorphous silicon dioxide ($6.025 \mu\text{m}$ thick) – thick line. The applied illumination intensity ranged from 0.9 to $10 \mu\text{W}/\text{cm}^2$.

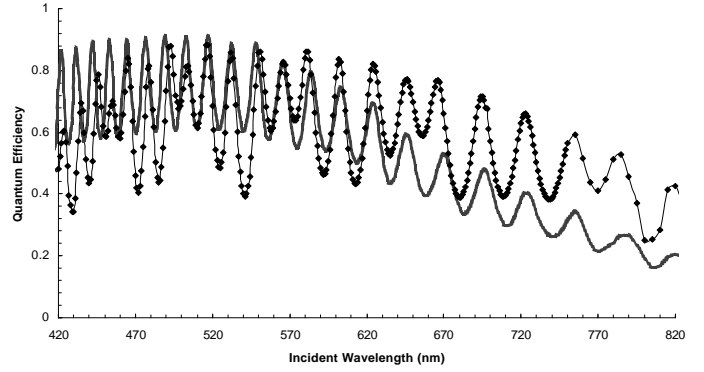


Fig. 2. (a) Measured external quantum efficiency of n^+p_{epi} photodiode – thin line with data points; (b) Theoretical quantum efficiency based on epitaxial collection only – thick line.

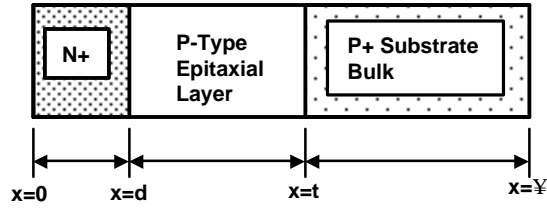


Fig. 3. A simple depiction of one-dimensional n^+p_{epi} type photodiode.

$$J_{ph} = qG_o L_{op} (\exp(-d/L_{op}) - \exp(-t/L_{op})) + q\Phi_s$$

$$\Phi_s = G_o L_{op} L_s \exp(-t/L_{op}) \left(\frac{L_s - L_{op}}{L_s^2 - L_{op}^2} \right) - \frac{D_s N_e}{L_s N_s} \hat{n}_e(t)$$

$$\hat{n}_e(t) = \frac{G_o L_{op}}{D_e} \left(\frac{L_{op} \exp(-d/L_{op}) (1 - \exp(-t/L_{op}))}{-t \exp(-t/L_{op}) \left(1 - L_s \left(\frac{L_s - L_{op}}{L_s^2 - L_{op}^2} \right) \right)} \right)$$

simplifies to

$$J_{ph} = qG_o L_{op} \left(\exp(-d/L_{op}) - L_{op} \exp(-t/L_{op}) \left(\frac{L_s - L_{op}}{L_s^2 - L_{op}^2} \right) \right)$$

Fig. 4. The simplification of the photocurrent expression following the simplification of the high-low junction by an ideal carrier sink. The shown solution of photocarrier flux across the epitaxial-substrate interface, F_s , reduces to its first term in the case the high-low junction is approximated by an ideal carrier sink.

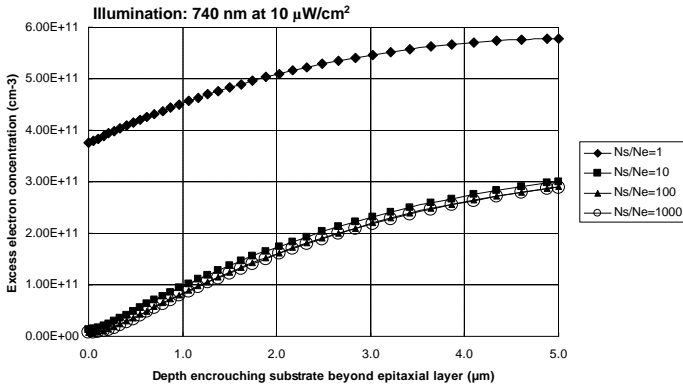


Fig. 5. The excess electron concentration profile in the substrate as a function of the substrate to epitaxial doping ratio (N_s/N_e) obtained by device simulation using *Medici*. The employed parameters were extracted from a standard $0.35 \mu\text{m}$ CMOS process.

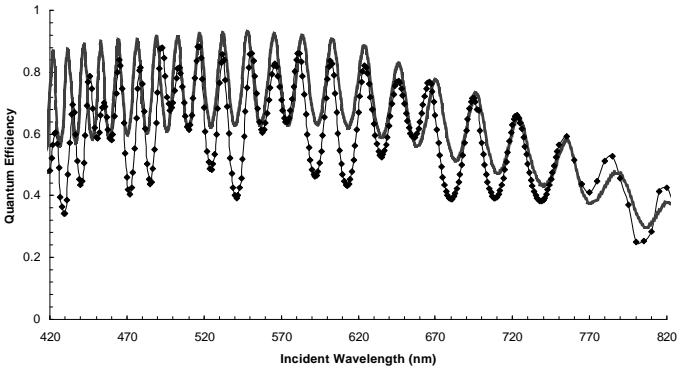
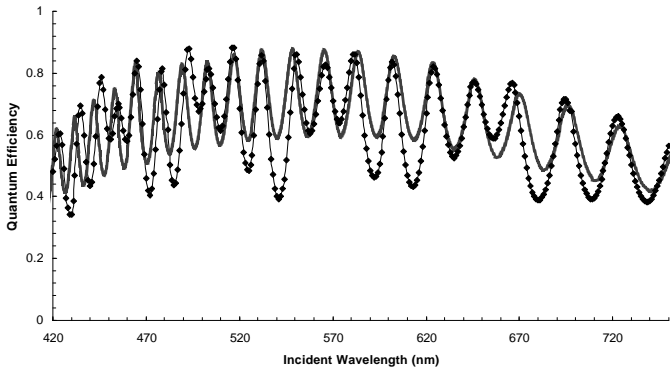


Fig. 6. (a) Measured external quantum efficiency of n^+p_{epi} photodiode – thin line with data points; (b) Semi-empirical quantum efficiency fitted by varying substrate diffusion length (at $L_{s,\text{fitted}} = 3.0 \mu\text{m}$) – thick line

Fig. 7. (a) Measured external quantum efficiency of n^+p_{epi} photodiode – thin line with data points; (b) Final expression of quantum efficiency with empirical parameters (at $L_{s,\text{fitted}} = 3.0 \mu\text{m}$ and $d_{\text{fitted}} = 50 \text{nm}$) – thick line.